Korean J. Chem. Eng., **26**(3), 603-611 (2009)

Dynamics and stability of ethylene polymerization in multizone circulating reactors

Nayef Mohamed Ghasem*,†, Wee Lee Ang, and Mohamed Azlan Hussain*****

*Department of Chemical & Petroleum Engineering, UAE University, Al Ain, P.O. Box 17555, UAE
**VSR Automation S/B, 3, Jalan Astaka U8/83, Section U8, Bukit Jelutong Industrial Park, 40150 Shah Alam, Selangor, Malaysia,
***Department of Chemical Engineering, University of Malaya, 50603 Kuala Lumpur, Malaysia
(*Received 15 November 2007 • accepted 28 October 2008*)

Abstract−Multizone circulating bed reactors (MZCR) have the exclusive characteristics of producing polymers of different molecular weights in a single particle. Traditional fluidized bed reactors, on the other hand, can produce only one kind of molecular weight with relatively narrow distribution. A dynamic model for the MZCR is used to illustrate the basic dynamic behavior of the new reactor design used for polyethylene production. The model is used to study the copolymerization of ethylene with butene. Several parameter sensitivity analyses are performed to show the computer-simulated time responses for reactor temperature, number-average molecular weight, weight-average molecular weight, catalyst feed rate and the monomer/comonomer concentration along the reactor length. At certain operating conditions dynamic instability is observed and the results for the effect of cooling water temperature, catalyst feed rate, monomer and comonomer initial feed concentration on the reactor temperature and polymer molecular weight reveal that the system is very sensitive to disturbances in the heat exchanger coolant temperature. Also, at some operating conditions, the reactor temperature oscillates above the polymer melting temperature. Temperature runaway above polymer softening point is a serious problem which may cause polymer melting and hence reactor shutdown. The oscillatory behavior of the reactor temperature necessitates a suitable temperature control scheme to be installed.

Key words: Polyethylene, Multi Zone Circulating Reactor, Ethylene, Polymerization

INTRODUCTION

Polyethylene is currently the largest tonnage plastic in the world, covering almost half of the total usage of thermoplastics [1]. Being the most popular type of polymer, it has received considerable attention from researchers in both industries and academia. Since the first industrial production of polyethylene in 1938, there have been many innovative designs of catalytic and reactor systems, and these have led to a better production economy and increased production capacity [2]. At the same time, the polymer structure is carefully engineered so that the production of polyethylene with tailor-made physicomechanical properties is possible. And it has been shown that by conducting polymerization in two or more polymerization steps, polymer properties could be definitely expanded [3]. However, there is a problem associated with these multi-step processes. The polymer produced has low homogeneity.

The new technology developed by Basell uses a multizone circulating reactor (MZCR) (Fig. 1) to produce polymer with an onion ring structure. MZCR was first reported in the open literature by Govoni et al. [4] and Covezzi and Mei [3], in which they comprehensively discussed the rationale of the idea, design of the reactor, and expected outputs from the new design, such design simplicity, efficient heat removal, high specific productivity, and low energy consumption. The reactor configuration enables polymerization to be carried out in two polymerization zones realized by two cylindrical interconnected vertical legs, termed riser and downer, respectively. In the riser section, the polymer flows upward by means fast fluidization or pneumatic transport. The gas is fed in the bottom of the riser section along with polymer particles coming from the downer

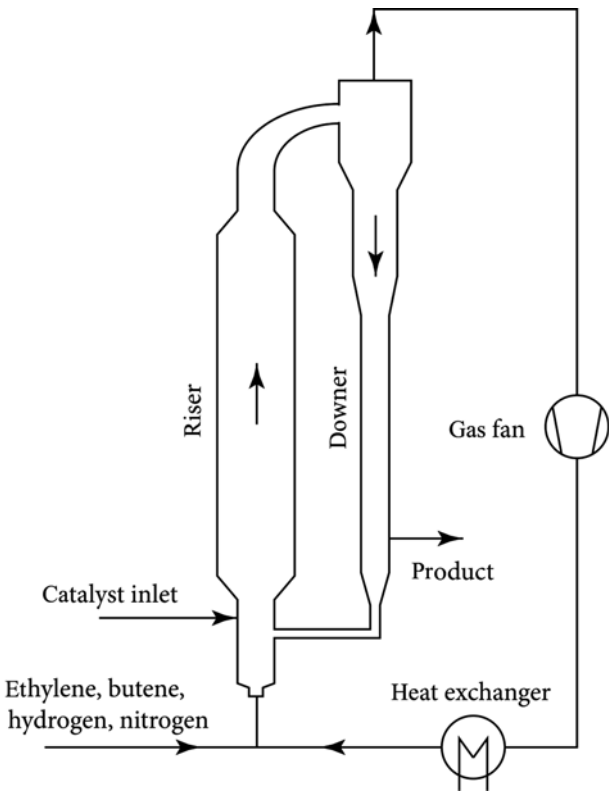

Fig. 1. Process configuration of the MZCR.

†To whom correspondence should be addressed.
E-mail: nayef@uaeu.ac.ae

section and prepolymer or catalyst made up of active sites. The polymer particles leaving the riser section are transferred to the cyclone positioned in the top of the downer section. In the cyclone, the polymer particles are separated from the gas stream and fall to the downer section, through which the polymer particles flow in packed bed mode under action of gravity.

Despite many novel features offered by the MZCR technology, theoretical and experimental studies on MZCR in the open literature are lacking, and only a few modeling studies are available. Santos et al. [5] first considered an isothermal, dynamic mathematical model for the MZCR, which takes into account particle and reactor levels, as well as the particle population balance. This model is capable of predicting polymer productivity, particle size distribution, molecular weights, and polydispersity of the polymer. Their main result is that the molecular weight distribution can be narrowed by decreasing the recycle ratio or increasing the hydrogen ratio in the riser and downer. Based on a simplified kinetic model developed by McAuley et al. [6], Fernandes and Lona [7] described a steady-state and isothermal reactor model for the MZCR. They conducted several simulations with their model to investigate typical reactor behavior. Parameter sensitivity studies were also performed for the effects of inert concentration: catalyst feed rate, gas velocity and voidage in the riser, and downer bed height on polymer properties. Simulation studies were also performed in the case when a gas barrier is introduced in the top of the downer section. In the present paper, the steady-state model of Fernandes and Lona [7] is extended and turned into a dynamic model so that the transient behavior of the MZCR can be simulated. Also, the isothermal condition imposed by Santos et al. [5] and Fernandes and Lona [8] is relaxed in this study.

KINETIC MECHANISM

When supported catalyst particles are injected into the polymerization reactor, the chemical species in Table 1 take part in a series of complex reactions at the interface between the solid catalyst and the polymer matrix. The reaction begins by the formation of active sites, which is assumed to take place in excess of cocatalyst [6,9-12]. This reaction is followed by an initiation reaction, in which the monomer gases and the active sites are combined to form live polymers. The live polymers then grow according to the propagation reactions. Most dead polymer are produced by chain transfer reactions which can occur in several ways. For simplicity, only chain transfer to monomers and hydrogen is considered in the kinetic modeling. The Arrhenius equations for the kinetic constants are given in Table 2, in which the preexponential constants are calculated by using data from McAuley et al. [6] and Hatzantonis et al. [13]. Direct use of the kinetic mechanism and the rate expressions would give rise to an unmanageably large number of differential equations in the mathematical model of the reactor. It is therefore desirable if the kinetics and rate expressions could be manipulated to a simpler form. Employing the method of pseudokinetic rate constant [14], the kinetic mechanism summarized in Table 1 may be viewed as if it is equivalent to the pseudokinetic mechanism in Table 3.

Table 1. Reaction mechanisms

Type of reaction	Kinetic mechanism	Pseudokinetic mechanism
Activation	$R \xrightarrow{k_n} P_0$	$R \xrightarrow{k_n} P_0$
Initiation	$P_0 + M_j \xrightarrow{k_{i,j}} P_{1,j}$	$P_0 + M \xrightarrow{k_i} \mu_0$
Propagation	$P_{n,i} + M_j \xrightarrow{k_{p,ij}} P_{n+1,j}$	$\mu_0 + M \xrightarrow{k_p} \mu_0$
Monomer chain transfer	$P_{n,i} + M_j \xrightarrow{k_{f,ij}} P_{1,j} + Q_n$	$\mu_0 + M \xrightarrow{k_f} P_1 + v_0$
Hydrogen chain transfer	$P_{n,i} + H_2 \xrightarrow{k_{h,i}} P_0^* + Q_n$	$\mu_0 + H_2 \xrightarrow{k_h} P_0^* + v_0$

Table 2. Kinetic rate constants

Rate constants	Unit
$k_n = 7.19557 \times 10^4 \exp(-8000/1.987T)$	1/s
$k_{i,1} = 2.91205 \times 10^5 \exp(-9000/1.987T)$	L/(mol s)
$k_{i,2} = 4.07687 \times 10^4 \exp(-9000/1.987T)$	L/(mol s)
$k_{h,1} = 6.33210 \times 10^3 \exp(-8000/1.987T)$	L/(mol s)
$k_{h,2} = 6.33210 \times 10^3 \exp(-8000/1.987T)$	L/(mol s)
$k_{p,11} = 2.47524 \times 10^7 \exp(-9000/1.987T)$	L/(mol s)
$k_{p,12} = 5.82409 \times 10^5 \exp(-9000/1.987T)$	L/(mol s)
$k_{p,21} = 1.86371 \times 10^7 \exp(-9000/1.987T)$	L/(mol s)
$k_{p,22} = 4.36807 \times 10^5 \exp(-9000/1.987T)$	L/(mol s)
$k_{f,11} = 1.51107 \times 10^2 \exp(-8000/1.987T)$	L/(mol s)
$k_{f,12} = 4.31734 \times 10^2 \exp(-8000/1.987T)$	L/(mol s)
$k_{f,21} = 1.51107 \times 10^2 \exp(-8000/1.987T)$	L/(mol s)
$k_{f,22} = 4.31734 \times 10^2 \exp(-8000/1.987T)$	L/(mol s)

Table 3. Pseudokinetic rate constants

Kinetic parameters
$k_i = ([M_1]k_{i,1} + [M_2]k_{i,2})/([M_1] + [M_2])$
$k_{p,1} = ([M_1]k_{p,21}k_{p,11} + [M_2]k_{p,12}k_{p,21})/([M_1]k_{p,21} + [M_2]k_{p,12})$
$k_{p,2} = ([M_1]k_{p,21}k_{p,12} + [M_2]k_{p,12}k_{p,22})/([M_1]k_{p,21} + [M_2]k_{p,12})$
$k_p = ([M_1]k_{p,1} + [M_2]k_{p,2})/([M_1] + [M_2])$
$k_{f,1} = ([M_1]k_{f,21}k_{f,11} + [M_2]k_{f,12}k_{f,21})/([M_1]k_{f,21} + [M_2]k_{f,12})$
$k_{f,2} = ([M_1]k_{f,21}k_{f,12} + [M_2]k_{f,12}k_{f,22})/([M_1]k_{f,21} + [M_2]k_{f,12})$
$k_f = ([M_1]k_{f,1} + [M_2]k_{f,2})/([M_1] + [M_2])$
$k_h = ([M_1]k_{p,21}k_{h,1} + [M_2]k_{p,12}k_{h,2})/([M_1]k_{p,21} + [M_2]k_{p,12})$

DYNAMIC MODEL

From elementary material and energy balances, a dynamic model for the MZCR can be derived, with the following assumptions: (i) the fluid flow is plug flow with no radial gradients and axial dispersion, (ii) the bed voidage and superficial velocity of gas and solids are invariant with respect to time and space along the bed, (iii) the polymerization reactions take place only in the solid phase, (iv) heat effects due to activation, initiation, and chain transfers are neglected [7,8]. The model consists of 12 partial differential equations. The catalyst consumption is governed by the equations on potential active sites and active sites, which are

$$\frac{\partial [R]}{\partial t} + v_{solid}\frac{\partial [R]}{\partial z} = -k_n[R] \quad (1)$$

$$\frac{\partial [P_0]}{\partial t} + v_{solid}\frac{\partial [P_0]}{\partial z} = k_n[R] - k_i[P_0][M] \quad (2)$$

where $[M]=[M_1]+[M_2]$. The concentrations of ethylene (j=1), butane

(j=2), and hydrogen are given by

$$\frac{\varepsilon}{1-\varepsilon}\left(\frac{\partial[M_j]}{\partial t}+v_{gas}\frac{\partial[M_j]}{\partial z}\right)=-(k_{i,j}[P_0]+k_{p,j}\mu_0+k_{f,j}\mu_0)[M_j] \quad (3)$$

$$\frac{\varepsilon}{1-\varepsilon}\left(\frac{\partial[H_2]}{\partial t}+v_{gas}\frac{\partial[H_2]}{\partial z}\right)=-k_h\mu_0[H_2] \quad (4)$$

The live and dead moment equations for the characterization of the polymers are

$$\frac{\partial\mu_m}{\partial t}+v_{solid}\frac{\partial\mu_m}{\partial z}=k_i[P_0][M]-k_h\mu_m[H_2]+(1-\delta_m)[M]\left(k_p\sum_{j=1}^{m-1}\frac{m!}{j!(m-j)!}+k_f(\mu_0-\mu_m)\right) \quad (5)$$

$$\frac{\partial v_m}{\partial t}+v_{solid}\frac{\partial v_m}{\partial z}=(k_f[M]+k_h[H_2])\mu_m \quad (6)$$

where δ_m is the discrete delta function. The reactor temperature considers the enthalpy change in both the solid and gas phases:

$$(\varepsilon[G]C_{p,gas}+(1-\varepsilon)\rho_{pol}C_{p,pol})\frac{\partial T}{\partial t}+(\varepsilon v_{gas}[G]C_{p,gas}+(1-\varepsilon)v_{solid}\rho_{pol}C_{p,pol})\frac{\partial T}{\partial z}=(-\Delta H_{rxn})k_p\mu_0[M](1-\varepsilon) \quad (7)$$

where $[G]=[M]+[H_2]+[N_2]$ and $C_{p,gas}=(C_{p,M_1}[M_1]+C_{p,M_2}[M_2]+C_{p,N_2}[N_2]+C_{p,H_2}[H_2]/[G]$.

1. Initial and Boundary Conditions

The partial differential equations are solved with a set of initial boundary conditions. For the initial conditions, it is assumed that the reactor is initially empty and at a temperature of T_0. For the boundary conditions, the effects of catalyst and polymer recirculation from the downer to the riser are considered in the following equations:

$$[R]|_{z=0}^{(r)}=[R]|_{z=L}^{(d)}+[R]|_{makeup} \quad (8)$$

$$([P_0]\ \mu_i\ v_i)|_{z=0}^{(r)}=([P_0]\ \mu_i\ v_i)|_{z=L}^{(d)} \quad (9)$$

As the gas species are consumed slowly in the riser, their concentration at the feed line is assumed to be time invariant. The temperature of the gas-solid mixture at the feed line,

$$T|_{z=0}^{(r)}=f(T|_{z=L}^{(d)},T_R) \quad (10)$$

considers the contribution of the enthalpies at the downer bottom and the cooled recycled gas temperature T_R

$$V_{hex}[G]C_{p,gas}\frac{\partial T_R}{\partial t}=\varphi_{recycle}v_{gas}^{(r)}[G]C_{p,gas}A_R(T|_{z=0}^{(r)}-T_R)-UA(T_R-T_w) \quad (11)$$

where V_{hex} is the heat exchanger volume, A_R is the cross sectional area of the reactor.

2. Hydrodynamics

A simple plug flow model is assumed both in the riser and the downer of the reactor [8]. For the riser section of the reactor, fast fluidizing condition is assumed, and the Haider-Levenspiel equation [15] is used to relate the solid and gas velocities:

$$v_{solid}^{(r)}=v_{gas}^{(r)}-\frac{\mu_{gas}}{\rho_{gas}d_p}\frac{Ar}{18+0.591Ar^{1/2}} \quad (12)$$

The hydrodynamics in the downer is closely related to that of the riser. Material balance requires solid velocities in riser and downer to be related by

$$v_{solid}^{(d)}=\left(\frac{1-\varepsilon^{(r)}}{1-\varepsilon^{(d)}}\right)v_{solid}^{(r)} \quad (13)$$

The gas velocity in downer, on the hand, is given by

$$v_{gas}^{(d)}=(1-\varphi_{recycle})v_{gas}^{(r)} \quad (14)$$

The leading moments (m=0, 1, 2) are used in the calculation of weight average molecular weight M_w and number average molecular weight M_n

$$M_n=\left(\frac{\mu_1+v_1}{\mu_0+v_0}\right)\frac{W_1[M_1]+V_2[M_2]}{[M_1]+[M_2]} \quad (15)$$

$$M_w=\left(\frac{\mu_2+v_2}{\mu_1+v_1}\right)\frac{W_1[M_1]+V_2[M_2]}{[M_1]+[M_2]} \quad (16)$$

where W_1 and W_2 are the molecular weights of the monomer and comonomer, respectively.

3. Numerical Solution

The set of partial differential equations describing the reactor can be solved by reducing them to a set of ordinary differential equations by approximating the spatial derivative with the following first-order finite difference:

$$\frac{\partial[\ldots]}{\partial z}=\frac{[\ldots]_{i+1}-[\ldots]_{i-1}}{\Delta z} \quad (17)$$

which divides the reactor into N equally spaced subreactors (Fig. 2) where $N=L/\Delta z$. The discretized model equations are as follows:

$$\frac{d[R]}{dt}=\frac{v_{solid}}{\Delta z}([R]|_{in}-[R])-k_n[R] \quad (18)$$

$$\frac{d[P_0]}{dt}=\frac{v_{solid}}{\Delta z}([P_0]|_{in}-[P_0])+k_n[R]-k_i[P_0][M] \quad (19)$$

$$\frac{d[M_j]}{dt}=\frac{v_{gas}}{\Delta z}([M_j]|_{in}-[M_j])-(k_{i,j}[P_0]+k_{p,j}\mu_0+k_{f,j}\mu_0)[M_j]\left(\frac{1-\varepsilon}{\varepsilon}\right),$$

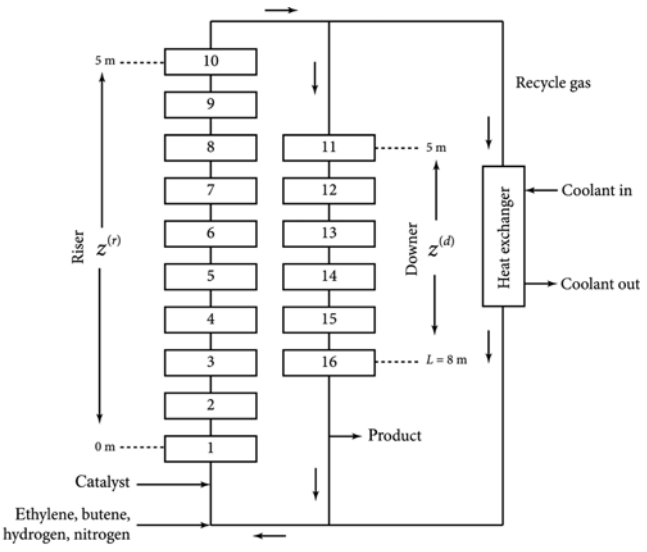

Fig. 2. Discretized model of the MZCR.

$$j=1,2 \quad (20)$$

$$\frac{d[H_2]}{dt}=\frac{v_{gas}}{\Delta z}([H_2]|_{in}-[H_2])+k_h\mu_0[H_2]\left(\frac{1-\varepsilon}{\varepsilon}\right) \quad (21)$$

$$\frac{d\mu_0}{dt}=\frac{v_{solid}}{\Delta z}(\mu_0|_{in}-\mu_0)+k_i[P_0][M]-k_h\mu_0[H_2] \quad (22)$$

$$\frac{d\mu_1}{dt}=\frac{v_{solid}}{\Delta z}(\mu_1|_{in}-\mu_1)+k_i[P_0][M]-k_h\mu_1[H_2]+k_p\mu_0[M]+k_f(\mu_0-\mu_1)[M] \quad (23)$$

$$\frac{d\mu_2}{dt}=\frac{v_{solid}}{\Delta z}(\mu_2|_{in}-\mu_2)+k_i[P_0][M]-k_h\mu_2[H_2]+k_p(2\mu_1+\mu_0)[M]+k_f(\mu_0-\mu_2)[M] \quad (24)$$

$$\frac{d\nu_j}{dt}=\frac{v_{solid}}{\Delta z}(\nu_j|_{in}-\nu_j)+(k_f[M]+k_h[H_2])\mu_j,\ \ j=0,1,2 \quad (25)$$

$$\frac{dT}{dt}=\frac{\varepsilon[G]C_{p,gas}v_{gas}+(1-\varepsilon)\rho_{pol}C_{p,pol}v_{solid}}{\Delta z(\varepsilon[G]C_{p,gas}+(1-\varepsilon)\rho_{pol}C_{p,pol})}(T|_{in}-T)+\frac{(-\Delta H_{rxn})k_p[M]\mu_0(1-\varepsilon)}{\varepsilon[G]C_{p,gas}+(1-\varepsilon)\rho_{pol}C_{p,pol}} \quad (26)$$

SIMULINK is the modeling environment for simulating the reactor model; the numerical solution of the blocks in SIMULINK uses the MATLAB's numerical ODE solver in for stiff systems, ode15s (Bogacki-Shampine algorithm). For the numerical solution of the model, the discretized equations for the riser and downer sections are implemented in Matlab as two m-fles, namely riser.m and downer.m, which are essentially the same except in the definitions of solid/gas velocities and bed voidage. Another two m-files, risersf.m and downersf.m, are required so that the equations coded in riser.m and downer.m can be called to an S-function block in SIMULINK. The dynamic model is used to study the effect of operating conditions such as coolant temperature, catalyst flow rate, catalyst potential and active sites concentration, ethylene/butene concentrations on the reactor temperature, number average and weight average molecular weight, polydispersity and molecular weight distribution. Since under industrial conditions it is very difficult to maintain coolant temperature and catalyst feed rate constant, a sine wave function was considered to represent coolant temperature to the heat exchanger and catalyst feed rate.

Table 4. Operating conditions used in the simulations

Parameters	Values
a_c	0.548 mmol/g
$[M_1]_0$	0.30 mol/liter
$[M_2]_0$	0.10 mol/liter
$[H_2]_0$	0.02 mol/liter
$[N_2]_0$	0.65 mol/liter
C_{p,M_1}	46 J/mol/K
C_{p,M_2}	100 J/mol/K
C_{p,H_2}	28 J/mol/K
C_{p,N_2}	27 J/mol/K
$C_{p,pol}$	1.839 J/g/K
ρ_{gas}	29 kg/m^3
$(-\Delta H_{rxn})$	94.5 kJ/mol
d_p	500 m
q	0.2 g/s
ρ_{pol}	950 kg/m^3
μ_{gas}	11.6 μPa·s

Table 5. Parameters and initial conditions for ethylene polymerization

Parameters	Values
$z^{(r)}$	0 (bottom) to 5 m (top)
$z^{(d)}$	5 (top) to 8 m (bottom)
D	0.3 m
$\varepsilon^{(r)}$	0.90
$\varepsilon^{(d)}$	0.15
$v_{gas}^{(r)}$	5 m/s
$\varphi_{recycle}$	0.9
T_0	330 K
T_w	303 K
V_{hex}	0.1 m^3
UA	0.3 kW/K

RESULTS AND DISCUSSION

Based on the nominal operating conditions and parameters [8,16] listed in Tables 4 and 5, simulations were conducted to show the typical dynamic behavior of the considered reactor. The effect of the operating conditions on the system behavior was investigated.

1. Ethylene and Butene Concentrations

Ethylene is the main monomer for the production of high density polyethylene (HDPE) and linear low density polyethylene (LLDPE). In the production of LLDPE, comonomer such as butene or hexane is introduced to add side branches on the main polymeric chain. In the present work, butene is used as comonomer to modify the polymer properties. Fig. 3 depicts the change in the ethylene concentration versus reaction time and reactor length. From the figure it is obvious that the ethylene concentration decreases with time because of the continuous growth of the polymerization reaction, hence increase in ethylene consumption rate.

Butene depleting rate is depicted in Fig. 4. There is a very slight

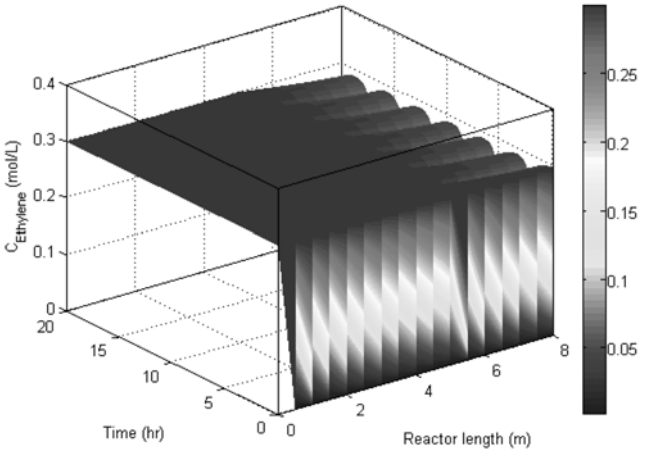

Fig. 3. Ethylene concentrations versus time and reactor length.

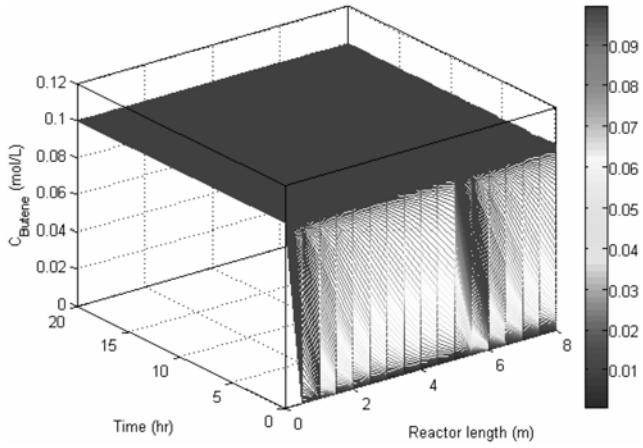

Fig. 4. Butene concentrations versus time and reactor length.

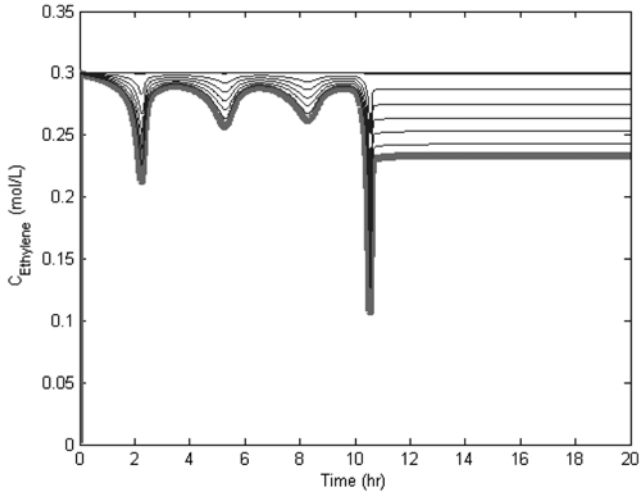

Fig. 5. Ethylene concentrations versus time at different spots in the reactor, catalyst feed rate from 0.2 g/s to 0.5 g/s after 10 hours of operation, solid line is at the exit of the downer.

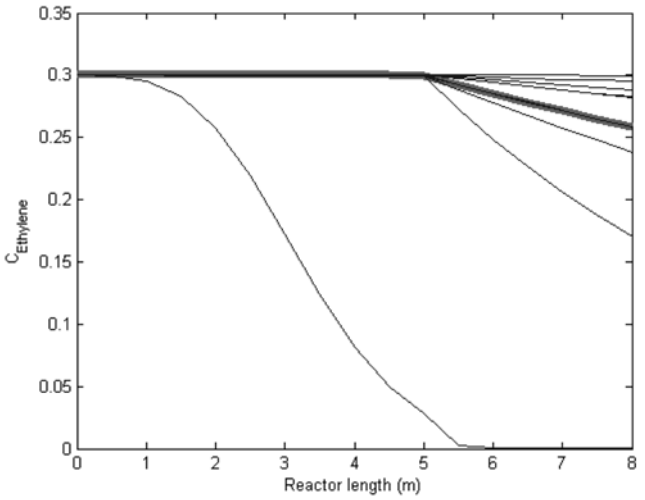

Fig. 6. Ethylene concentrations versus reactor length, solid line is at exit of the downer.

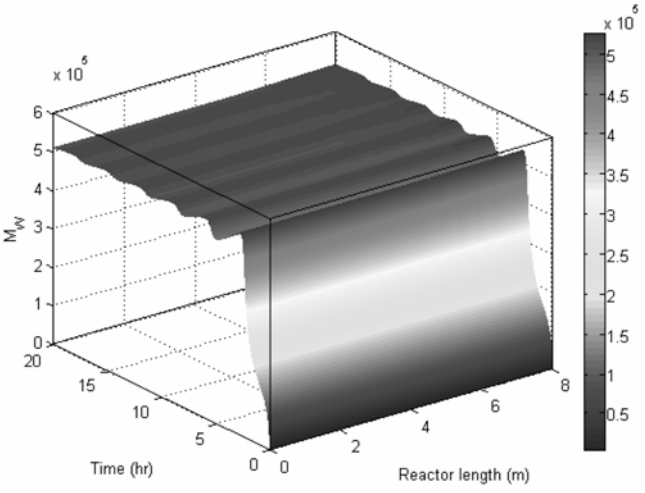

Fig. 7. Weight-average molecular weight (Mw) versus time and reactor length.

drop in the butene concentration with time compared to that of ethylene concentration in the downer because of low reactivity of butane as compared to that of ethylene. Low consumption of ethylene or low polymerization rate in the riser is due to high gas and solid velocities and hence the short gas residence time. Conversely, in the downer, the ethylene consumption rate is high because of low gas velocity, low porosity and longer gas residence time. The ethylene concentration rate at the given operating conditions (Tables 4 and 5) in the downer is not stable as can be noticed from the oscillations depicted in Fig. 3.

The oscillations depicted in the butene concentration at the end of the downer are negligible as can be seen close to the end of the downer (Fig. 4). The instability behavior can be shown by raising the catalyst feed rate, say, 0.2 g/s to 0.5 g/s (Fig. 5) after 10 hours of operation; it clear from the diagram that the concentation drops sharply before reaching steady state as the catalyst feed rate is increased. Ethylene concentration versus time and reactor length is portrayed in Fig. 6. The diagram gives an idea about the change in ethylene concentration through the riser is almost negligible. There is a significant drop in the ethylene concentration through the downer; the steady state path is the one in strained in solid thick line.

2. Molecular Weight and Molecular Weight Distribution

For a polymer to be practical it must have transition temperatures above room temperatures and mechanical properties sufficient to bear design loads. Fig. 7 describes the changes in weight average molecular weight (M_w) versus the reactor length and reaction time. The diagram demonstrates that the change in the weight average molecular with time at any specific spot in the reactor is unstable as can be seen from the oscillatory performance of the system. The stable steady state cannot be attained throughout the 20 hours of operation. This shows that the system is operating under unstable steady state operating circumstances.

A convenient parameter that characterizes the extent of the molecular weight distribution is the polydispersity, which is the ratio of weight-average molecular weight to the number-average molecular weight. Fig. 8 plots the polydispersity index of the polymer versus time and reactor length. As the polymerization reaction goes to com-

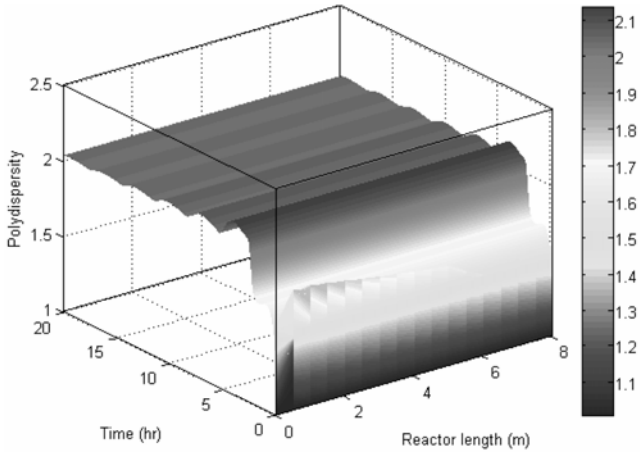

Fig. 8. Polydispersity profiles.

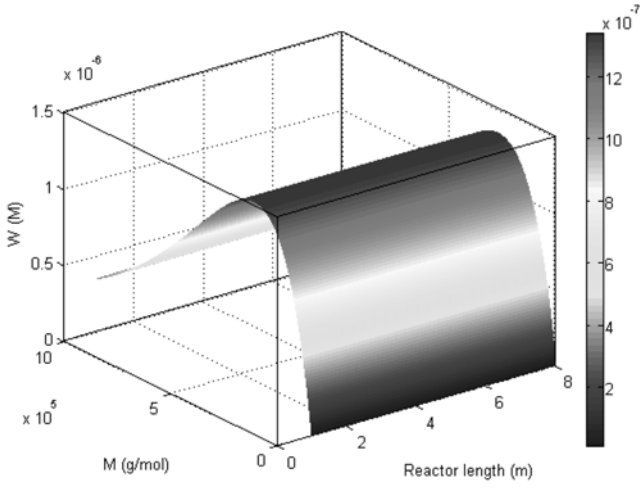

Fig. 9. Molecular weight distributions at H_2 concentration of 0.02 mol/L, 0.3 mol/L ethylene.

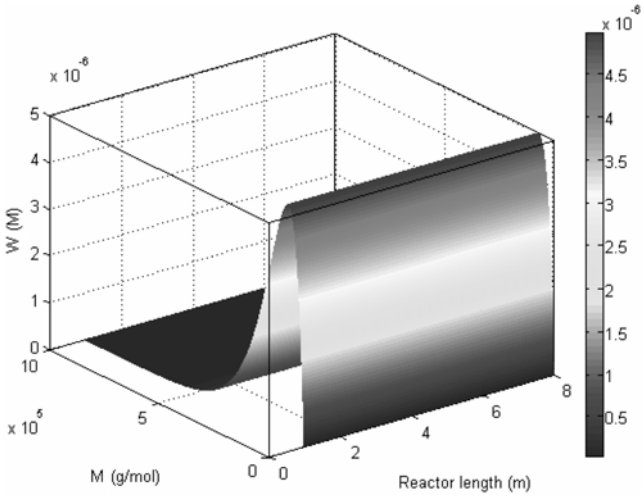

Fig. 10. Molecular weight distribution for H_2 concentration of 0.2 mol/L, 0.3 mol/L ethylene.

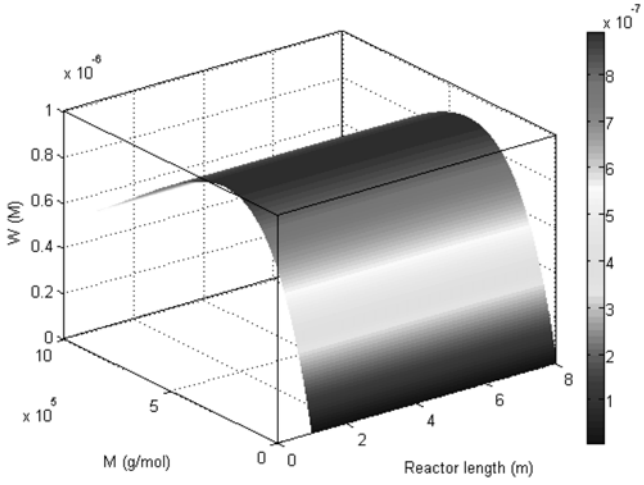

Fig. 11. Molecular weight distribution for ethylene concentration of 0.5 mol/L, H_2 0.02 mol/L.

pletion, polydispersity swings around a value of 2. The diagram brings to light that the polydispersity is oscillating slightly with time. At a preset reactor length, the polydispersity index increases with time until it reaches a value of 2. Measurement of the molecular weight distribution is useful when a polymer property depends not just on the number of polymer molecules but on the size or weight of each polymer.

Molecular weight distribution at hydrogen concentration of 0.02 mol/L is shown in Fig. 9 at other fixed operating conditions (Table 4). The different molecular weight produced in the riser and the downer leads to a polymer with broad molecular weight distribution. Fig. 10 illustrates the effect of hydrogen concentration on the molecular weight distribution as hydrogen concentration increases starting from 0.02 mol/L raised to 0.2 mol/L. The polymer produced at this high hydrogen concentration has narrow molecular weight distribution, because hydrogen terminates the polymer chains, hence producing polymers with low molecular weight. Ethylene concentration also has a significant effect on the molecular weight distribution. Fig. 11 represents the molecular weight distribution at high ethylene concentration (i.e., 0.5 mol/L). The diagram reveals that as the ethylene concentration increases, polymer reaction rate increases, hence molecular weight increases. A broader molecular weight distribution is observed with the increase in the ethylene concentration.

3. Reactor Temperature

Control of reactor temperature is one of the most crucial state variables in fluidized and circulating bed reactors for polyethylene production. Because ethylene polymerization is highly exothermic, the temperature of the polymer tends to rise and sometimes it will exceed the polymer melting point; at high temperatures polymer particles can become sticky and during collisions can form large agglomerates that can possibly undergo sintering and cause de-fluidization. In the opposite situation, if the bed is too cold, the particles can become brittle and may fracture forming unwanted small fragments that elutriate with the gas. Hence, heat and mass transfer to the particle surface controls the local particle temperature and the rates of agglomeration and breakage. The reactor temperature profile as a function of time and reactor length is depicted in Fig. 12. At a specific reactor length, the reactor temperature oscillates with

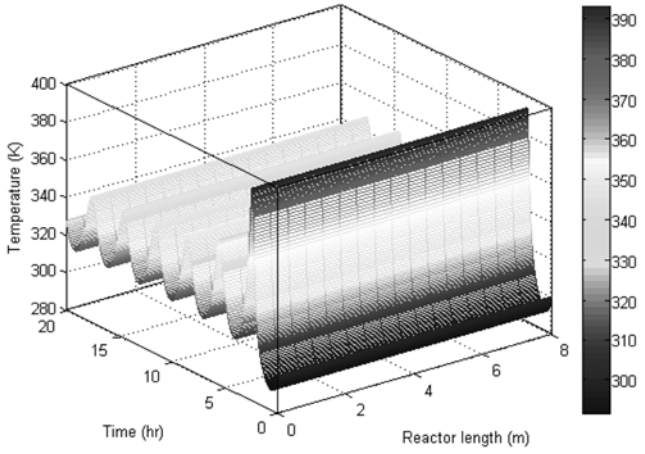

Fig. 12. Reactor temperature versus time and reactor length at catalyst feed rate of 0.2 g/s.

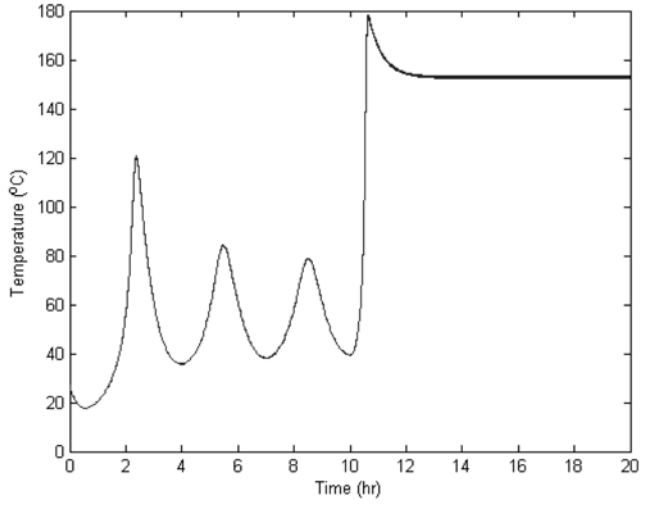

Fig. 13. Reactor temperature time trajectories after a step change in catalyst feed rate from 0.2 g/s to 0.5 g/s at fixed other conditions.

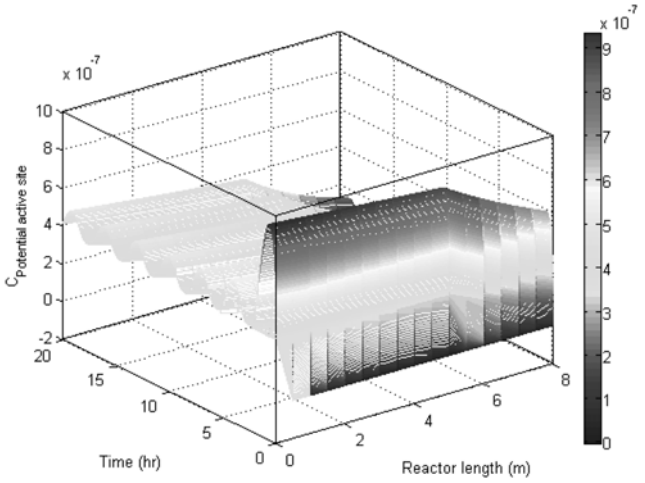

Fig. 14. Potential active site concentration versus time and reactor length at 0.2 g/s catalyst feed rate.

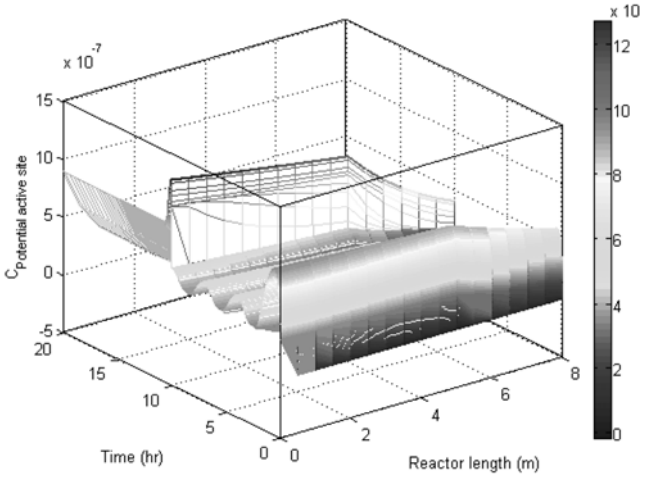

Fig. 15. Potential active site concentration after a step change in catalyst feed rate from 0.2 to 0.5 g/s after a time of 10 hours of operation.

time. This reveals that at the given operating condition the reactor falls under unstable steady state operating conditions. The increase of the temperature all the way in the riser is irrelevant; by contrast there is a significant increase in the downer temperature, and the increase in the reaction temperature in the downer is a result of the increase in the rate polymerization, consequently an increase in the rate of heat released. Fig. 13 depicts the reactor temperature versus time and reactor length after a step change in catalyst feed rate. The reactor starts with catalyst feed rate of 0.2 g/s; during this stage the temperature is oscillating constantly. After 10 hours of operation a step change in catalyst feed rate to 0.5 g/s results in increasing the reactor temperature to 370 K and the temperature achieves a steady state situation. The diagram discloses that the change in the temperature profile throughout the riser is unimportant, whereas the temperature increased somewhat along the downer. The increase in the catalyst feed rate caused immediate overshot in the reactor temperature and changed the reactor temperature from unstable steady state to stable steady state.

4. Catalyst Active and Potential Active Sites

Fresh catalysts consist of potential active sites, and co-catalyst is fed continuously to the reactor; interaction between them results in the formation of vacant active sites. Fig. 14 depicts the concentration of the catalyst potential active sites versus time and reactor length. From the diagram it can be seen that the system is unstable. The potential active site decreases slightly through the riser; on the other hand, there is a sharp decrease in the downer section of the reactor because of the continuous formation of the active sites. The effect of catalyst feed rate on the system behavior is examined by a step change in the catalyst feed rate from 0.2 g/s to 0.5 g/s after 10 hours of operation. The unstable steady state disappears after a swift overshoot in the potential active concentration because of the impulsive addition of the fresh catalyst, then oscillation vanishes and a stable steady state is perceived (Fig. 15).

Fig. 16 shows the catalyst active site concentration versus reactor length and time. It can be noticed that the concentration of the active sites oscillates with time throughout the reactor length. The

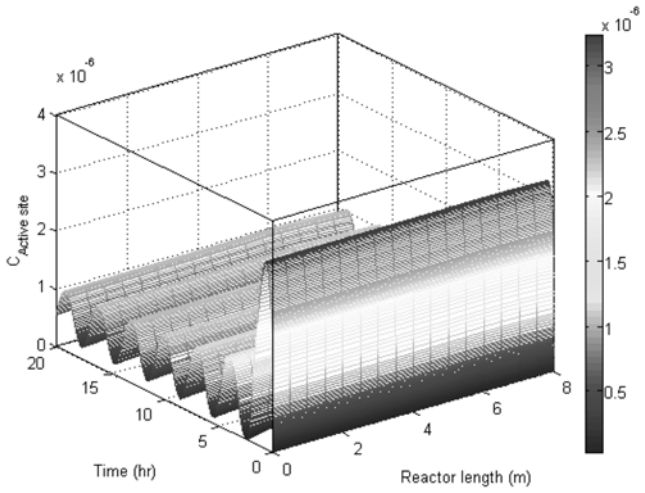

Fig. 16. Active site concentrations versus time at different locations inside the reactor.

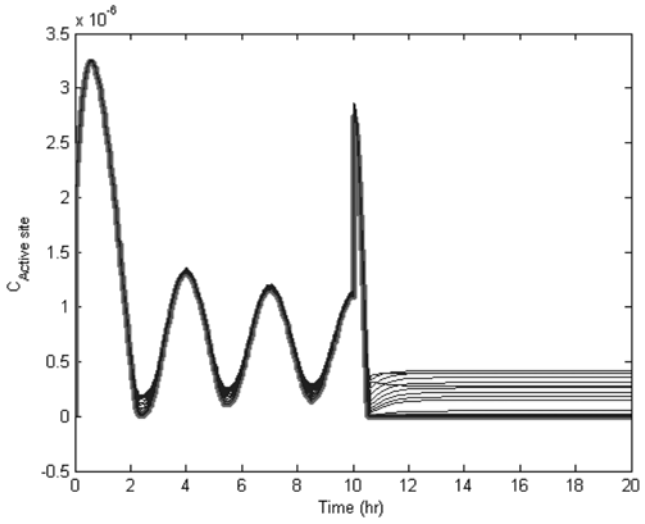

Fig. 17. Active site for step change in catalyst feed rate from 0.2 to 0.5 g/s after 10 hours of operation, solid red line is at the exit of the downer.

generated vacant active site concentration increases slightly at the very beginning, then starts to decline with time because of the continuous progress in the polymerization reaction. As the number of active sites decreases, consequently its concentration decreases, which was a result of the long residence time in the downer section and hence the increases in the polymerization reaction rate. Fig. 17 illustrates the catalyst active site concentration versus reactor length and time, after a step change in catalyst feed rate. It is clear that the oscillatory manners of the active site break up in a steady state form at a step change in the catalyst feed rate from 0.2 to 0.5 g/s. The rate of the decrease in the concentration of the catalyst active sites in the riser is insignificant compared to the downer. In the downer section of the reactor, the consumption rate of the potential active site is higher than that of the riser due to the increase in the reaction rate as a result of long residence time and low porosity. Fig. 18 shows the catalyst active site concentration versus reactor length and time;

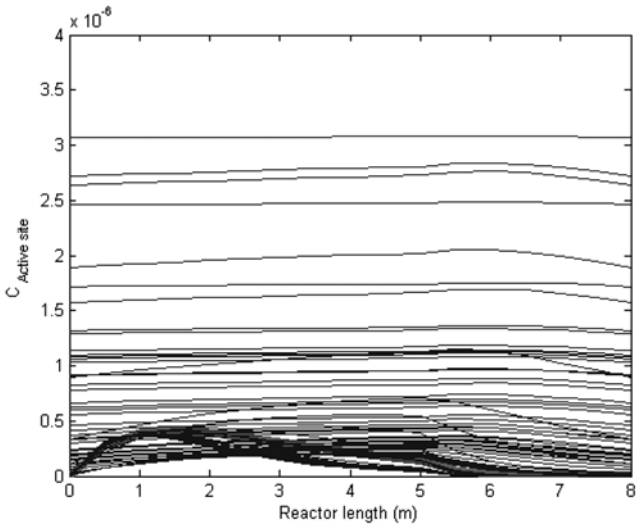

Fig. 18. Catalyst active site versus reactor length for a step change in catalyst feed rate from 0.2 to 0.5 g/s after 10 hours of operation.

the steady state profile is shown with solid line. The diagram shows that there is a slight increase in the catalyst active site concentration at the inlet of the reactor due to the continuous formation of active sites and the low polymerization reaction rate. In the downer section of the reactor, the consumption rate of the catalyst active sites is higher than the formation rate; for that reason there is a continuous decrease in the active site concentration through the length of the downer.

CONCLUSIONS

A steady-state model of the MZCR for polyethylene production has been successfully extended to a dynamic model that incorporates the time domain. The mathematical model of the MZCR consists of a set of partial differential equations. The model equations were reduced to ordinary differential equations by using finite difference method. The set of the ordinary differential equations were solved in SIMULINK/MATLAB environment. Computer simulations were performed to illustrate the typical dynamic behavior of the reactor and parametric investigations of the effects of catalyst feed rate, catalyst potential and active site concentrations, monomer and comonomer concentrations, reactor temperature and molecular weights. The model is suitable for the implementation of automatic control of the important reactor operating variables such as reactor temperature, polymer molecular weight and molecular weight distribution which previously could not be achieved by using the steady-state model.

NOMENCLATURE

a_c : catalyst active site concentration [mmol/g]
Ar : Archimedes number, dimensionless
A_R : cross sectional area of the reactor [m^2]
C_{p,M_1} : ethylene heat capacity [J/mol/K]
C_{p,M_2} : butene heat capacity [J/mol/K]

C_{p,H_2} : hydrogen eat capacity [J/mol/K]
C_{p,N_2} : nitrogen heat capacity [J/mol/K]
$C_{p,pol}$: polymer heat capacity [J/mol/K]
D : reactor diameter [m]
d_p : polymer particle diameter [mm]
[G] : total gas concentration [mol/liter]
$(-\Delta H_{rxn})$: heat of reaction [kJ/mol]
H_2 : chain transfer agent (hydrogen) concentration [mol/liter]
$[H_2]_0$: hydrogen feed concentration [mol/liter]
L : total reactor length (riser and downer) [m]
M_i : olefin monomer (i=1 for ethylene, 2=butene)
M_n : number-average molecular weight [g/mol]
M_w : weight-average molecular weight [g/mol]
$[M_i]_0$: monomer feed concentration [mol/liter (i=1 for ethylene, 2=butene)]
N : number of subreactors
$[N_2]_0$: nitrogen feed concentration [mol/liter]
$P_{n,i}$: live polymer with chain length n, terminal type i
Q_n : dead polymer with chain length n [mol/liter]
q : catalyst feed rate [g/s]
R : potential active site (inactive catalyst site)
T : reaction temperature [K]
T_0 : initial reactor temperature [K]
T_R : recycle gas temperature [K]
T_w : heat exchanger inlet coolant temperature [K]
UV : heat transfer parameter
V_{hex} : heat exchanger volume [m^3]
$v_{gas}^{(r)}$: gas velocity in the riser [m/s]
$v_{solid}^{(r)}$: solid velocity in the riser [m/s]
$v_{gas}^{(d)}$: gas velocity in the downer [m/s]
$v_{solid}^{(d)}$: solid velocity in the downer [m/s]
$z^{(r)}$: riser length [m]
$z^{(d)}$: downer length [m]

Greek Letters

ρ_{pol} : polymer density [kg/m^3]
ρ_{gas} : gas density [kg/m^3]
μ_{gas} : gas viscosity [Pa·s]
$\varphi_{recycle}$: gas recycle ratio
μ_i : *i*-th live moment
v_i : *i*-th dead moment
$\varepsilon^{(d)}$: downer void fraction
$\varepsilon^{(r)}$: riser void fraction
δ_m : discrete delta function

REFERENCES

1. E. Benham and M. McDaniel, Ethylene polymers, HDPE, *in Encyclopedia of polymer science and technology*, H. Mark ed., Wiley, New York, 382-412 (2003).
2. H. Knuuttila, A. Lehtinen and A. N. Pakarinen, *Adv. Polym. Sci.*, **169**, 13 (2004).
3. M. Covezzi and G. Mei, *Chem. Eng. Sci.*, **56**, 4059 (2003).
4. G. Govoni, R. Rinaldi, M. Covezzi and P. Galli, *Process and apparatus for gas phase polymerization of α-olefins*, U.S. Patent, 5,698,642 (1997).
5. J. L. Santos, M. Vecino, E. Ochoteco, M. Montes and J. M. Asua, *Proc. 7th Int Workshop Polym. Reaction Eng.*, 155 (2001).
6. K. B. McAuley, J. F. MacGregor and A. E. Hamielec, *AIChE J.*, **36**, 837 (1999).
7. F. A. N. Fernandes and L. M. F. Lona, *J. Appl. Polym. Sci.*, **93**, 1053 (2004).
8. F. A. N. Fernandes and L. M. F. Lona, *J. Appl. Polym. Sci.*, **93**, 1042 (2004).
9. H. S. Cho, K. H. Choi, D. J. Choi and W. Y. Lee, *Korean J. Chem. Eng.*, **17**, 205 (2000).
10. H. S. Cho and W. Y. Lee, *Korean J. Chem. Eng.*, **19**, 557 (2002).
11. J. S. Chung, G. Tairova, Y. Zhang, J. C. Hsu, K. B. McAluley and D. W. Bacon, *Korean J. Chem. Eng.*, **19**, 597 (2002).
12. Y. G. Ko, H. S. Cho, K. H. Choi and W. Y. Lee, *Korean J. Chem. Eng.*, **16**, 562 (1999).
13. H. Hatzantonis, H. Yiannoulakis and A. Yiagopoulos, *Chem. Eng. Sci.*, **55**, 3237 (2000).
14. H. Tobita and A. H. Hamielec, *Polymer*, **32**(14), 2641 (1991).
15. D. Kunii and O. Levenspiel, *Chem. Eng. Sci.*, **52**, 2471 (1997).
16. N. M. Ghasem, *Chem. Eng. Technol.*, **22**(9), 777 (1999).